

LETTERS • OPEN ACCESS

# Suppression of single-wall carbon nanotube redox reaction by adsorbed proteins

To cite this article: Tomohito Nakayama *et al* 2018 *Appl. Phys. Express* **11** 075101

View the [article online](#) for updates and enhancements.

## Related content

- [Evaluation of the individualization state in single-walled carbon nanotube solutions using absorption, Raman and photoluminescence spectroscopy](#)  
Wonsuk Jung, Ju Yeon Woo, Seung Ho Lee et al.
- [Efficient separation of semiconducting single-wall carbon nanotubes by surfactant-composition gradient in gel filtration](#)  
Boanerges Thendie, Haruka Omachi, Yasumitsu Miyata et al.
- [Observing and predicting the preferential functionalization of metallic or semiconducting single-walled carbon nanotubes](#)  
Jimmy Nicolle, Xavier F. Le Goff, Agnès Grandjean et al.



## Suppression of single-wall carbon nanotube redox reaction by adsorbed proteins

Tomohito Nakayama<sup>1,2</sup>, Takeshi Tanaka<sup>2</sup>, Kentaro Shiraki<sup>1</sup>, Muneaki Hase<sup>1</sup>, and Atsushi Hirano<sup>2\*</sup>

<sup>1</sup>Division of Applied Physics, Faculty of Pure and Applied Sciences, University of Tsukuba, Tsukuba, Ibaraki 305-8573, Japan

<sup>2</sup>Nanomaterials Research Institute, National Institute of Advanced Industrial Science and Technology (AIST), Tsukuba, Ibaraki 305-8565, Japan

\*E-mail: [hirano-a@aist.go.jp](mailto:hirano-a@aist.go.jp)

Received March 27, 2018; accepted May 13, 2018; published online June 6, 2018

Single-wall carbon nanotubes (SWCNTs) are widely used in biological applications. In biological systems, proteins readily adsorb to SWCNTs. However, little is known about the effects of proteins on the physicochemical properties of SWCNTs, such as their redox reaction. In this study, we measured the absorption and Raman spectra of SWCNTs dispersed in the presence of proteins such as bovine serum albumin to observe the redox reaction of the protein-adsorbed SWCNTs. The adsorbed proteins suppressed the redox reaction by forming thick and dense layers around the SWCNTs. Our findings are useful for understanding the behaviors of SWCNTs in biological systems. © 2018 The Japan Society of Applied Physics

Carbon nanotubes are a type of nanoparticles that have been utilized for various applications on the basis of their unique chemical, mechanical, optical, and electrical properties.<sup>1–4</sup> In particular, a number of studies have attempted a variety of biological applications, including bio-imaging,<sup>5,6</sup> biosensing,<sup>7</sup> and drug transport.<sup>8,9</sup> The carbon nanotubes have been reported to induce oxidative stress in cells and proteins;<sup>10,11</sup> these reactions occur in biological systems through the redox reactions of the carbon nanotubes. Thus, clarification of the carbon nanotube reactivity in terms of their redox reactions in the presence of proteins is required to understand the physicochemical properties and biological impacts of carbon nanotubes in biological systems.

In general, the redox reactions of carbon nanotubes are altered by adsorbed solutes. Some surfactants, such as sodium deoxycholate and sodium dodecylbenzene sulfonate (SDBS), have been reported to substantially reduce the reactivity through the formation of thick and dense adsorbed layers around the carbon nanotubes.<sup>12,13</sup> In contrast, sodium dodecyl sulfate (SDS), which is a common surfactant, allows the redox reaction to occur owing to the sparse layer it forms around the carbon nanotubes.<sup>13</sup> The thickness and density of the adsorbed layers are thus important factors for determining the reactivity of carbon nanotubes in aqueous solutions.

In biological systems, the aromatic surfaces of carbon nanotubes do not remain exposed to the solvent; that is, carbon nanotubes interact with proteins through van der Waals, hydrophobic, and  $\pi$ - $\pi$  interactions between the sidewalls of the carbon nanotubes and the amino acid residues of the proteins.<sup>14–18</sup> The aromatic surfaces of the carbon nanotubes are therefore readily and nonspecifically coated by proteins, leading to the formation of protein layers called the protein corona.<sup>19</sup> Accordingly, the protein layers potentially affect the redox reactions of the carbon nanotubes, as was observed for surfactant solutions. However, little is known about the effects of adsorbed proteins on the redox reactions of carbon nanotubes.

In this work, we focused on the redox reaction of protein-adsorbed single-wall carbon nanotubes (SWCNTs) using bovine serum albumin (BSA) as a model protein. It was reported that the dispersion efficiency of the SWCNTs using BSA is affected by the pH-dependent conformational changes of BSA.<sup>20</sup> In addition, a previous thermodynamic study

showed that the adsorption capacity of BSA onto SWCNTs increases with increasing temperature and decreasing pH from neutral to acidic.<sup>21</sup> Despite such reports, it remains unclear how BSA molecules affect the redox reactions of the SWCNTs. In this study, the redox reaction was induced by changing the pH on the basis of the  $O_2/H^+/H_2O$  couple. SDS was used as a control dispersant, and the redox reaction was observed by absorption and Raman spectroscopies. This is the first report of proteins suppressing the redox reaction of SWCNTs more effectively than SDS, which is an indication of the thick and dense layer formed by proteins around the SWCNT surfaces; such adsorbed layers are even retained in solid form.

SWCNTs produced by the high-pressure catalytic CO decomposition (HiPco) process were dispersed at a concentration of 0.2 mg/mL in the presence of 2.0 mg/mL BSA or 2.0 mg/mL SDS by ultrasonication for 60 min at 18 °C and ca. 2 W/cm<sup>2</sup>, followed by ultracentrifugation (210,000g for 30 min at 25 °C). The BSA-dispersed SWCNT (SWCNT-BSA) and SDS-dispersed SWCNT (SWCNT-SDS) samples were collected from the supernatants and examined by absorption and Raman spectroscopies to characterize the SWCNT dispersion; note that absorption and Raman spectra were mainly used to determine the dispersibility and redox reaction of the semiconducting and metallic SWCNTs, respectively (see also the online supplementary data at <http://stacks.iop.org/APEX/11/075101/mmedia> for details of materials and methods).<sup>22,23</sup>

The absorption spectra of the SWCNT-BSA and SWCNT-SDS samples are shown in Fig. 1(a), normalized to the absorbance at 625 nm, which is insensitive to their redox reaction. The absorption peaks of the samples observed at approximately 940–1350 and 625–940 nm are assigned to the  $S_{11}$  and  $S_{22}$  optical transitions, respectively;<sup>24</sup> note that the absorption peaks at longer wavelengths in the  $S_{11}$  optical transition correspond to SWCNTs with larger diameters. The peaks at approximately 400–625 nm are assigned to the  $M_{11}$  optical transition.<sup>24</sup> The SWCNTs contained in both samples were found to be highly dispersed because the spectra showed fairly sharp peaks.<sup>22</sup> The concentration of the dispersed SWCNT-SDS sample was ca. 4 times higher than that of the dispersed SWCNT-BSA sample, which was determined from the absorbance at 625 nm without normalization. The dif-



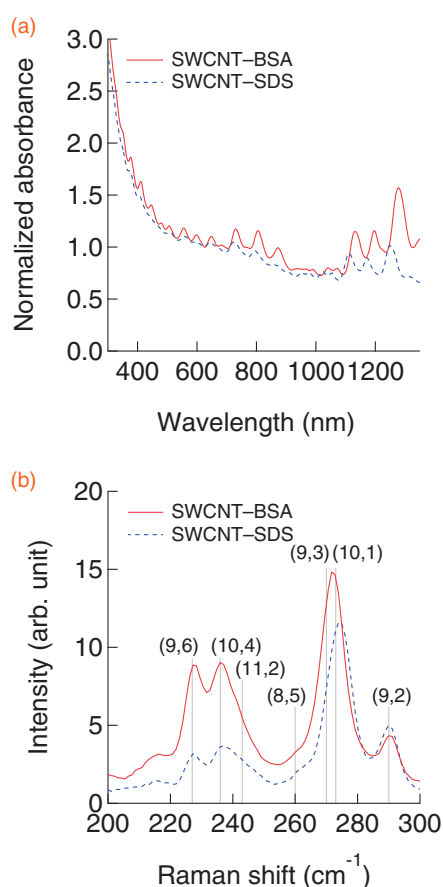


**Fig. 1.** (a) Absorption spectra of SWCNT-BSA and SWCNT-SDS samples normalized to the absorbance at 625 nm. (b) Raman spectra of SWCNT-BSA and SWCNT-SDS samples with an excitation wavelength of 532 nm. The peak positions were determined by decomposition using fitting by the Lorentzian function.

ferences in the respective peak positions between SWCNT-SDS and SWCNT-BSA are due to the difference in the dielectric constants in the vicinity of the SWCNTs.<sup>25,26</sup> Specifically, BSA provides a more hydrophilic environment than SDS in its interactions with the sidewalls of the SWCNTs.

Figure 1(b) shows the Raman spectra of the SWCNT-BSA and SWCNT-SDS samples in the radial breathing mode (RBM). The spectra were measured after diluting the samples to give identical concentrations of SWCNTs. Note that the excitation wavelength of 532 nm overlaps the optical transition of the metallic species in the SWCNTs.<sup>24</sup> The Raman spectra can be decomposed into several components by Lorentzian fitting, enabling the assignment of the peaks at 227, 236, 240, 260, 270, and 273  $\text{cm}^{-1}$  to (9, 6), (10, 4), (11, 2), (8, 5), (9, 3), and (10, 1) SWCNTs,<sup>27,28</sup> respectively, corresponding to metallic species; the peak at 290  $\text{cm}^{-1}$  was assigned to (9, 2) SWCNTs, corresponding to semiconducting species.<sup>28</sup> Note that the Raman peaks observed at lower wavenumbers correspond to SWCNTs with larger diameters because the diameter of the SWCNTs is expressed by  $d_t = 248/\omega_{\text{RBM}}$ ,<sup>29</sup> where  $d_t$  (nm) and  $\omega_{\text{RBM}}$  ( $\text{cm}^{-1}$ ) denote the diameter and the Raman shift in the RBM, respectively, of a SWCNT. Because the peak positions for the SWCNT-BSA sample are the same as those for the SWCNT-SDS sample, these dispersants nonselectively disperse every SWCNT.

Note that weaker spectral intensities were observed for SWCNT-SDS than for SWCNT-BSA in the absorption and Raman spectra, especially for the SWCNTs with larger diameters [Fig. 1(a)]. This phenomenon can be explained by the effect on SWCNT oxidation in aqueous solution through the redox chemistry of the  $\text{O}_2, \text{H}^+/\text{H}_2\text{O}$  couple.<sup>30,31</sup> Note that SWCNTs with larger diameters have a tendency to be more readily oxidized owing to their narrow band gaps.<sup>30,31</sup> In fact, the peak intensities of the SWCNT-SDS sample were reported to be restored by the addition of sodium deoxycholate, which has the ability to exclude dissolved oxygen molecules from the sidewalls of the SWCNTs,<sup>12</sup> thereby reinforcing the above interpretation. Thus, BSA molecules were found to effectively suppress the redox reaction of SWCNTs. We will show the suppression of the SWCNT redox reaction by BSA in detail, referring to the results of a systematic experiment described below.

We investigated the redox reaction of SWCNTs through the  $\text{O}_2, \text{H}^+/\text{H}_2\text{O}$  couple in the pH range of 2–11 by adding HCl or NaOH. As the proton concentration increased with decreasing pH, the redox potential of the  $\text{O}_2, \text{H}^+/\text{H}_2\text{O}$  couple increased,<sup>30,31</sup> which in turn caused electron withdrawal from the SWCNTs, i.e., oxidation or hole doping of the SWCNTs.<sup>30,31</sup> The absorbance spectra of the SWCNT-BSA and SWCNT-SDS samples are shown in Figs. 2(a) and 2(b), respectively. All peak intensities in the  $S_{11}$  transition were unambiguously attenuated at lower pH values, which is an indication of SWCNT oxidation. Note that the peak intensities of the SWCNT-BSA sample were better retained than those of the SWCNT-SDS sample, even under acidic conditions such as pH 3. The three major peaks in the  $S_{11}$  optical transition were labeled peaks I, II, and III from the side of the peak at longer wavelengths, as shown in Figs. 2(a) and 2(b). Typically, peak I corresponds to (9, 5), (8, 7), and (10, 5) SWCNTs, peak II corresponds to (8, 6) SWCNTs, and peak III corresponds to (8, 4), (7, 6), and (9, 4) SWCNTs.<sup>32</sup> Figures 2(c)–2(e) show the pH dependence of the three peak intensities for the SWCNT-BSA and SWCNT-SDS samples. The inflection points, i.e., midpoints, of the curves determined from sigmoidal fits were approximately 2 pH units lower for SWCNT-BSA than for SWCNT-SDS at all three wavelengths (Table I). Thus, BSA clearly suppresses the oxidation of the semiconducting SWCNTs. In addition, the midpoints followed the order peak I > peak II > peak III (Table I), which is consistent with the redox mechanism; specifically, SWCNTs with a small  $S_{11}$  transition energy tend to have electrons at higher energy levels in the valence band.<sup>31</sup> Furthermore, the fact that the attenuated peak intensities were restored by the addition of NaOH also supports the redox mechanism (see Fig. S1 in the online supplementary data at <http://stacks.iop.org/APEX/11/075101/mmedia>). Nevertheless, there is still a possibility that the pH dependence of the spectra is attributable to changes in the amount of adsorbed BSA molecules. It has been reported that the adsorbability of BSA onto SWCNTs is enhanced with decreasing pH from neutral to acidic owing to the conformational changes of BSA.<sup>20</sup> Another study also showed that the adsorption capacity of BSA onto SWCNTs increased with decreasing pH.<sup>21</sup> However, if the amount of adsorbed BSA on the SWCNTs had increased at acidic pH values in the present system, the spectral intensities would have increased owing to

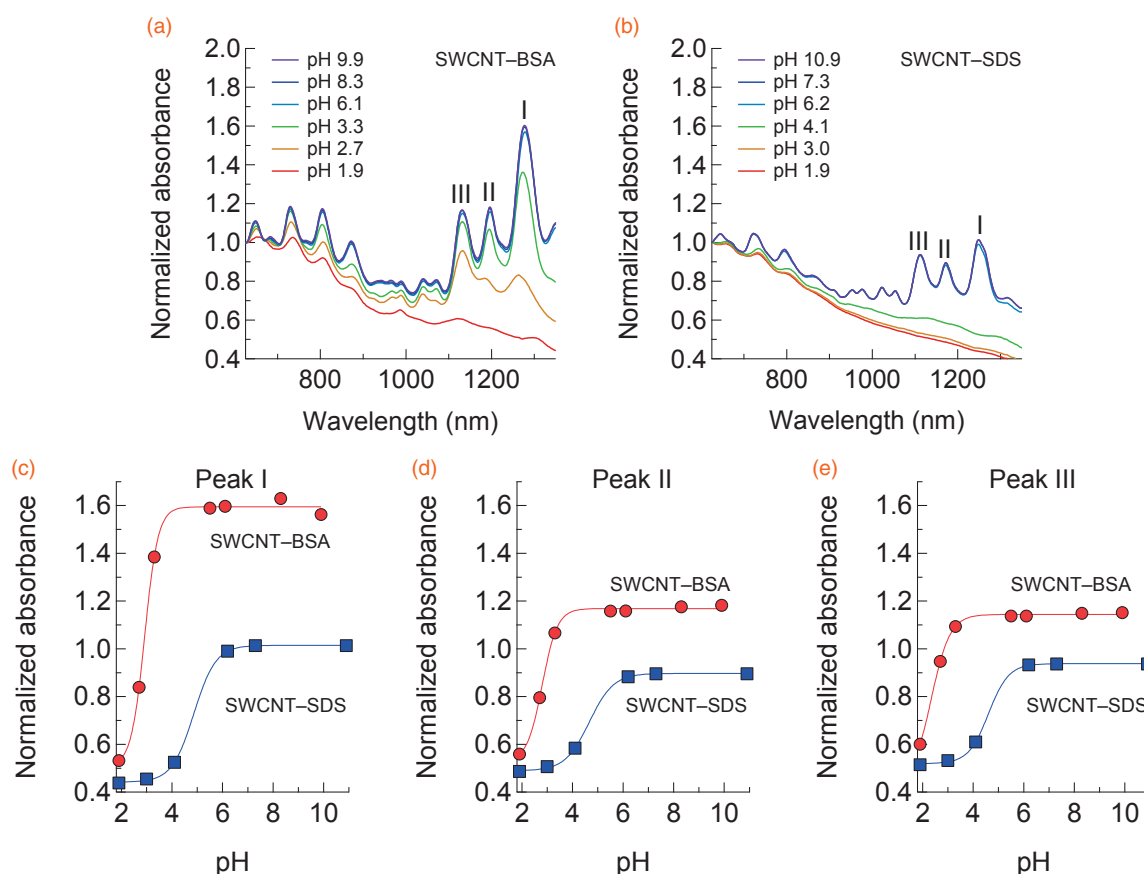


**Fig. 2.** pH dependence of the absorbance spectra of SWCNT-BSA (a) and SWCNT-SDS (b), which were normalized to the absorbance at 625 nm. Normalized absorbances of SWCNT-BSA and SWCNT-SDS at peaks I (c), II (d), and III (e) as a function of pH.

**Table I.** Midpoints of the pH-dependent absorption of SWCNT-BSA and SWCNT-SDS. The midpoints were determined from the sigmoidal fits shown in Figs. 2(c)–2(e).

Sample	Peak I	Peak II	Peak III
SWCNT-BSA	$2.92 \pm 0.04$	$2.80 \pm 0.03$	$2.34 \pm 0.11$
SWCNT-SDS	$4.87 \pm 0.05$	$4.66 \pm 0.06$	$4.61 \pm 0.09$

the exclusion of the dissolved oxygen molecules from the sidewalls of the SWCNTs, as mentioned above. The observed attenuation of the spectral intensities is thus derived from the redox reaction.

We also measured the Raman spectra of the SWCNT-BSA and SWCNT-SDS samples with an excitation wavelength of 532 nm at different pH values to investigate the redox reaction of the metallic SWCNTs. Note that the absorption spectra of the metallic SWCNTs are generally insensitive to the oxidation owing to a lack of their band gaps.<sup>28)</sup> Because these spectra were obtained by the resonance Raman scattering of the SWCNTs, the spectral intensities were significantly attenuated by the oxidation of the SWCNTs.<sup>12,28)</sup> The Raman spectral intensities of the SWCNT-BSA and SWCNT-SDS samples decreased with decreasing pH [Figs. 3(a) and 3(b)]. Importantly, the intensities of the SWCNTs with large diameters, e.g., the (9, 6) and (10, 4) SWCNTs, more readily decreased at acidic pH values than did the SWCNTs with smaller diameters, e.g., the (9, 3) and (9, 2) SWCNTs. Thus, the attenuation of the spectral intensities is clearly caused by the oxidation of the metallic SWCNTs, and it is concluded that BSA suppresses the oxidation of the metallic SWCNTs.

A similar trend was also observed in the Raman spectra with an excitation wavelength of 785 nm for the semiconducting SWCNTs (see Fig. S2 in the online supplementary data at <http://stacks.iop.org/APEX/11/075101/mmedia>).

As shown above, BSA molecules more pronouncedly suppress the SWCNT oxidation caused by the  $O_2/H^+/H_2O$  couple than do SDS molecules through their adsorption onto the sidewalls of the SWCNTs. Importantly, the absorption spectral intensities of the SWCNT-SDS sample were altered by the addition of BSA (see Fig. S3 in the online supplementary data at <http://stacks.iop.org/APEX/11/075101/mmedia>), which is an indication of the adsorption of BSA onto the SWCNTs. This result supports the suggestion that BSA has a higher affinity for the sidewalls of the SWCNTs than does SDS. The generality of such an effect on the suppression of oxidation was confirmed by using other oxidants, i.e., NaClO and  $K_2IrCl_6$  (see Fig. S4 in the online supplementary data at <http://stacks.iop.org/APEX/11/075101/mmedia>). The molecular size of BSA is approximately 5 nm,<sup>33)</sup> so the layers of BSA adsorbed on the SWCNTs appear to be sufficient to prevent electron transfer. It was also reported that BSA molecules accumulated on the SWCNT surface layer by layer.<sup>34)</sup> We thus concluded that BSA has a significantly high affinity for the SWCNTs and hence forms thick and dense adsorbed layers on the SWCNTs in the same way as some kinds of surfactants, such as sodium deoxycholate and SDBS,<sup>12,13)</sup> which suppress the redox reaction of the SWCNTs. If the surfaces of the SWCNT-BSA had remained exposed to the solvent like that of the SWCNT-SDS, they would have been oxidized more readily than what



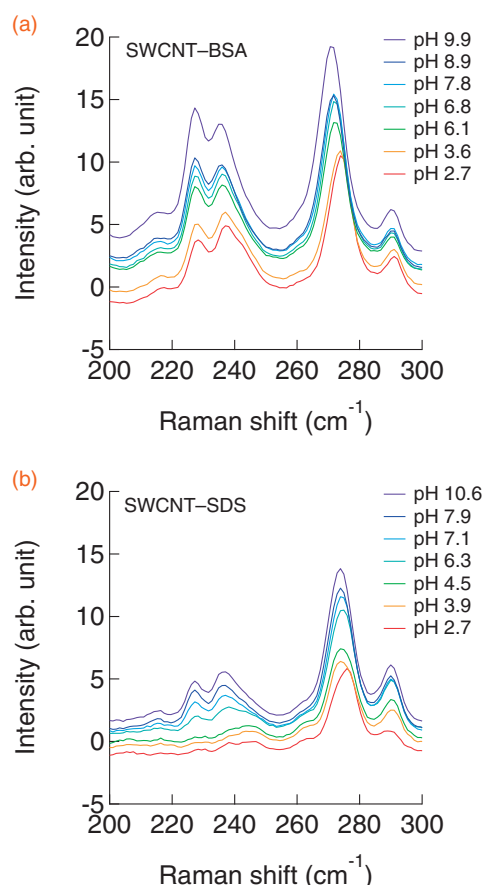


**Fig. 3.** Raman spectra of SWCNT-BSA (a) and SWCNT-SDS (b) with an excitation of wavelength of 532 nm as a function of pH.

was observed. In addition, this suppression of SWCNT oxidation through the  $O_2/H^+$ / $H_2O$  couple was observed in other systems that used other proteins, such as hen egg white lysozyme and chicken egg ovalbumin (see Fig. S5 in the online supplementary data at <http://stacks.iop.org/APEX/11/075101/mmedia>).

Proteins adsorbed more strongly to the SWCNTs than did SDS, forming stable adsorbed layers. To further confirm the high stability of protein adsorption on the SWCNTs, we examined the tolerance of the SWCNT-BSA sample to bundling, which was induced on a membrane by suction filtration to form a thin film; this approach is based on the concept that a dispersant with a higher affinity to SWCNTs leads to a higher dispersibility of the SWCNTs, even in a thin film. We also used SDBS-dispersed SWCNT (SWCNT-SDBS) as a control sample in this experiment; SDBS was reported to suppress the redox reaction because of its higher affinity to SWCNTs.<sup>13</sup> Films of SWCNT-BSA, SWCNT-SDS, and SWCNT-SDBS were fabricated as follows. Briefly, the SWCNT-BSA, SWCNT-SDS, or SWCNT-SDBS complex was mixed in a 1 : 1 ratio with methanol to induce the association of the SWCNT complexes, where these dispersants themselves did not aggregate, and the mixture was subjected to suction filtration to form a film on a polycarbonate membrane. We assumed that methanol insignificantly alters the affinities of proteins for the SWCNTs because proteins moderately retain their secondary structures in 50% methanol;<sup>35</sup> specifically, methanol induces negligible additional adsorption or desorption of proteins under this

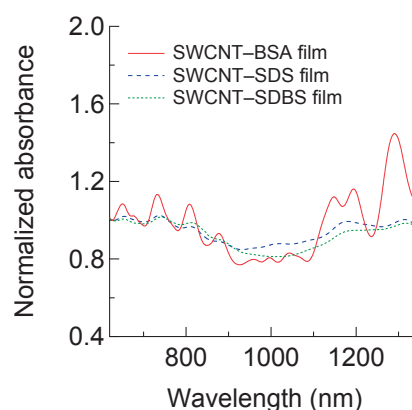


**Fig. 4.** Absorption spectra of SWCNT-BSA, SWCNT-SDS, and SWCNT-SDBS samples as films normalized to the absorbance at 625 nm.

condition. The absorption spectrum of the SWCNT-BSA film on a quartz glass substrate showed sharper peaks than those of the SWCNT-SDS and SWCNT-SDBS in the  $S_{11}$  and  $S_{22}$  transitions, even as a thin film (Fig. 4), which is an indication of the dispersion of SWCNT-BSA and the bundling of SWCNT-SDS and SWCNT-SDBS in the thin film.<sup>22</sup> Thus, it was confirmed that the BSA molecules form highly stable adsorbed layers around the SWCNTs in aqueous solutions and even in the thin film; such a high affinity of the BSA molecules for the SWCNTs accounts for the strong suppression of SWCNT oxidation exhibited by BSA.

In conclusion, we demonstrated that proteins highly disperse SWCNTs in aqueous systems and even in solid systems. Such high affinities of proteins for SWCNTs suppress the redox reaction of SWCNTs in aqueous solutions. The significant effects of proteins on SWCNTs are attributable to the thick and dense adsorbed layers formed by the proteins on the sidewalls of SWCNTs. These findings suggest that SWCNTs taken into biological systems undergo a reduction in reactivity in terms of their redox reaction through nonselective protein adsorption onto the SWCNTs. Thus, proteins can potentially deactivate the biological impacts of SWCNTs such as toxicity and the inflammatory effect through the adsorption reaction.

**Acknowledgments** This work was supported by JSPS KAKENHI Grant Number 18H01809, the Hosokawa Powder Technology Foundation, and Innovation School, General Affairs Headquarters, AIST, Japan.

- 1) Y.-P. Sun, K. Fu, Y. Lin, and W. Huang, *Acc. Chem. Res.* **35**, 1096 (2002).
- 2) M. Ma, F. Grey, L. Shen, M. Urbakh, S. Wu, J. Z. Liu, Y. Liu, and Q. Zheng, *Nat. Nanotechnol.* **10**, 692 (2015).
- 3) S. Kruss, A. J. Hilmer, J. Zhang, N. F. Reuel, B. Mu, and M. S. Strano, *Adv. Drug Delivery Rev.* **65**, 1933 (2013).
- 4) M. M. Shulaker, G. Hills, R. S. Park, R. T. Howe, K. Saraswat, H.-S. P. Wong, and S. Mitra, *Nature* **547**, 74 (2017).
- 5) Z. Liu, S. Tabakman, K. Welscher, and H. Dai, *Nano Res.* **2**, 85 (2009).
- 6) Y. Yomogida, T. Tanaka, M. Zhang, M. Yudasaka, X. Wei, and H. Kataura, *Nat. Commun.* **7**, 12056 (2016).
- 7) Z. Chen, S. M. Tabakman, A. P. Goodwin, M. G. Kattah, D. Daranciang, X. Wang, G. Zhang, X. Li, Z. Liu, P. J. Utz, K. Jiang, S. Fan, and H. Dai, *Nat. Biotechnol.* **26**, 1285 (2008).
- 8) A. A. Bhirde, V. Patel, J. Gavard, G. Zhang, A. A. Sousa, A. Masedunskas, R. D. Leapman, R. Weigert, J. S. Gutkind, and J. F. Rusling, *ACS Nano* **3**, 307 (2009).
- 9) S. F. Oliveira, G. Bisker, N. A. Bakh, S. L. Gibbs, M. P. Landry, and M. S. Strano, *Carbon* **95**, 767 (2015).
- 10) A. Hirano, T. Kameda, M. Wada, T. Tanaka, and H. Kataura, *J. Phys.*

- Chem. Lett. **8**, 5216 (2017).
- 11) C. Ge, Y. Li, J.-J. Yin, Y. Liu, L. Wang, Y. Zhao, and C. Chen, *NPG Asia Mater.* **4**, e32 (2012).
- 12) A. J. Blanch and J. G. Shapter, *J. Phys. Chem. B* **118**, 6288 (2014).
- 13) A. Hirano, T. Kameda, Y. Yomogida, M. Wada, T. Tanaka, and H. Kataura, *ChemNanoMat* **2**, 911 (2016).
- 14) M. Calvaresi and F. Zerbetto, *Acc. Chem. Res.* **46**, 2454 (2013).
- 15) G. Zuo, S. Kang, P. Xiu, Y. Zhao, and R. Zhou, *Small* **9**, 1546 (2013).
- 16) N. Yanamala, V. E. Kagan, and A. A. Shvedova, *Adv. Drug Delivery Rev.* **65**, 2070 (2013).
- 17) A. Antonucci, J. Kupis-Rozmyslowicz, and A. A. Boghossian, *ACS Appl. Mater. Interfaces* **9**, 11321 (2017).
- 18) A. Hirano, T. Tanaka, H. Kataura, and T. Kameda, *Chem.—Eur. J.* **20**, 4922 (2014).
- 19) C. Ge, J. Tian, Y. Zhao, C. Chen, R. Zhou, and Z. Chai, *Arch. Toxicol.* **89**, 519 (2015).
- 20) E. Edri and O. Regev, *Anal. Chem.* **80**, 4049 (2008).
- 21) T. Kopac and K. Bozgeyik, *Chem. Eng. Commun.* **203**, 1198 (2016).
- 22) M. J. O'Connell, S. M. Bachilo, C. B. Huffman, V. C. Moore, M. S. Strano, E. H. Haroz, K. L. Rialon, P. J. Boul, W. H. Noon, C. Kittrell, J. Ma, R. H. Hauge, R. B. Weisman, and R. E. Smalley, *Science* **297**, 593 (2002).
- 23) M. S. Strano, V. C. Moore, M. K. Miller, M. J. Allen, E. H. Haroz, C. Kittrell, R. H. Hauge, and R. E. Smalley, *J. Nanosci. Nanotechnol.* **3**, 81 (2003).
- 24) H. Kataura, Y. Kumazawa, Y. Maniwa, I. Umez, S. Suzuki, Y. Ohtsuka, and Y. Achiba, *Synth. Met.* **103**, 2555 (1999).
- 25) J. H. Choi and M. S. Strano, *Appl. Phys. Lett.* **90**, 223114 (2007).
- 26) A. G. Walsh, A. N. Vamvakas, Y. Yin, S. B. Cronin, M. S. Ünlü, B. B. Goldberg, and A. K. Swan, *Physica E* **40**, 2375 (2008).
- 27) M. S. Strano, S. K. Doorn, E. H. Haroz, C. Kittrell, R. H. Hauge, and R. E. Smalley, *Nano Lett.* **3**, 1091 (2003).
- 28) M. S. Strano, C. B. Huffman, V. C. Moore, M. J. O'Connell, E. H. Haroz, J. Hubbard, M. Miller, K. Rialon, C. Kittrell, S. Ramesh, R. H. Hauge, and R. E. Smalley, *J. Phys. Chem. B* **107**, 6979 (2003).
- 29) A. Jorio, R. Saito, J. H. Hafner, C. M. Lieber, M. Hunter, T. McClure, G. Dresselhaus, and M. S. Dresselhaus, *Phys. Rev. Lett.* **86**, 1118 (2001).
- 30) M. Zheng and B. A. Diner, *J. Am. Chem. Soc.* **126**, 15490 (2004).
- 31) A. Nish and R. J. Nicholas, *Phys. Chem. Chem. Phys.* **8**, 3547 (2006).
- 32) S. M. Bachilo, M. S. Strano, C. Kittrell, R. H. Hauge, R. E. Smalley, and R. B. Weisman, *Science* **298**, 2361 (2002).
- 33) B. X. Huang, H.-Y. Kim, and C. Dass, *J. Am. Soc. Mass Spectrom.* **15**, 1237 (2004).
- 34) C. Ge, J. Du, L. Zhao, L. Wang, Y. Liu, D. Li, Y. Yang, R. Zhou, Y. Zhao, Z. Chai, and C. Chen, *Proc. Natl. Acad. Sci. U.S.A.* **108**, 16968 (2011).
- 35) K. Matsuo, Y. Sakurada, S. Tate, H. Namatame, M. Taniguchi, and K. Gekko, *Proteins* **80**, 281 (2012).